PERSISTENT SCATTERER PROCESSING VALIDATION IN THE COURSE OF THE TERRAFIRMA PROJECT

Nico Adam[(1)], Alessandro Parizzi[(1)], Michael Eineder[(1)], Michele Crosetto [(2)]

(1) DLR, Oberpfaffenhofen, 82234 Wessling, Germany, nico.adam@dlr.de

(2) IG, Institute of Geomatics, 08860 Castelldefels, Spain, michele.crosetto@ideg.es

ABSTRACT

Terrafirma is an ESA project and a services element in the framework of the Global Monitoring for Environment and Security (GMES) service element programme. Based on the Persistent Scatterer Interferometry (PSI), the project provides a Pan European ground motion hazard information service. The motion monitoring is supplied by commercial companies which act as Operational Service Providers (OSPs).

A Product Validation Workgroup (PVW) has been formed for the validation and certification of the various motion data products which can provide different levels of value adding. Four OSPs operate processing chains for the generation of the basic level 1 product. These take part in a validation project which intends to demonstrate reliability and accuracy of the PSI motion monitoring. Amsterdam and Alkmaar in the Netherlands are the two test sites which are chosen for the comparison. Three data stacks - two from Envisat and one from ERS are processed independently by the OSPs in the course of the validation.

Two strategies for the validation are foreseen in the validation project: on the one hand the Product Validation and on the other the Process Validation. Both are independent and complementary to each other. The Product Validation utilizes available ground truth information for the validation and assesses the final geocoded motion data. The Process Validation is a new type of PSI validation and compares the intermediate data in slant range only and consequently avoids problems of geocoding, misregistration and interpolation. This comparison is made by the German Aerospace Center (DLR) with assistance of the Institute of Geomatics (IG) which leads the overall validation project. The new validation approach and the intermediate validation results are reported.

1 VALIDATION PRINCIPLE

The monitoring of the Earth's deformation effects with mm accuracy by PSI is a powerful but difficult estimation process. It includes long time span observations using a complex radar sensor, the coherent focussing of the radar acquisitions, the interferometrically processing of pairs of radar scenes and the separation of the phase contributions e.g. deformation, topography, atmospheric effects and noise. Fig. 1 provides a schematic visualisation of the signal and noise flow through the PSI-estimation subsystems. This processing principle can further be reduced into the standard estimation problem of the estimation of a signal (i.e. deformation) in additive noise which is visualized in Fig. 2.

The signal is the evolution in time of the distance of the stable scatter on ground to the radar sensor caused by a ground displacement. Noise is added by the object phase of the observed overall resolution cell (e.g. by clutter, temporal decorrelation and higher order scatters). Depending on the estimation principle, the atmospheric phase screen (APS) which is a deterministic signal actually needs to be considered to be noise. The performance of the overall PS estimation can be described by a bias and by the standard deviation of the estimation. A bias would describe a systematic effect. The standard deviation results from uncertainty and ambiguities in the measured values. Subject of DLR's work is the assessment of the actual performance of typical PSI processing chains, the check for systematic effects in the estimation and finally a validation including a qualification of the four participating OSPs. This process validation is limited to slant range geometry and measurements only.

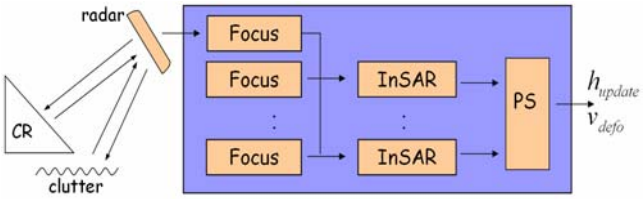

Fig. 1: Signal and noise flow in a PSI processing

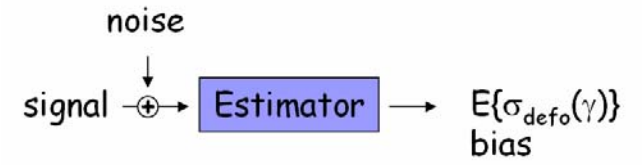

Fig. 2: Final principle of the above signal and noise flow applied in DLR's process validation

2 VALIDATION PREPARATIONS

The validation has been carefully prepared by the validation teams [1, 2 and 3]. This included for example the selection of the test sites regarding well known subsidence effects, the availability of usable radar acquisitions taking into account their temporal and baseline distribution and Doppler frequencies and a detailed specification of the deliveries and their data format and a definition of the initial DEM.

After the reception of the OSPs estimates the data were screened regarding the inter OSP coregistration which is the basis for the process validation. Moreover, each of the subsystems shown in Fig. 1 was checked for its specific error sources to guarantee correct input data in each subsystem. E.g.

- the focussing of the respective OSPs was checked in a procedure similar to the interferometric offset test [4]. In this check SLC scenes processed by ESA are used as the reference.
- The coregistration is considered the main error source in the interferometric processing. It was checked for systematic deviations in some scenes. The OSP's data were used without an external reference. Fig. 3 provides an example for the coregistration check.
- The PS detection can include wrong scatterers into the estimation process e.g. caused by sidelobes or higher order PS. Both effects were checked using DLR algorithms to detect sidelobes and to detect resolution cells with two dominant scatterers [5]. Fig. 9 provides an example for the sidelobe risk.

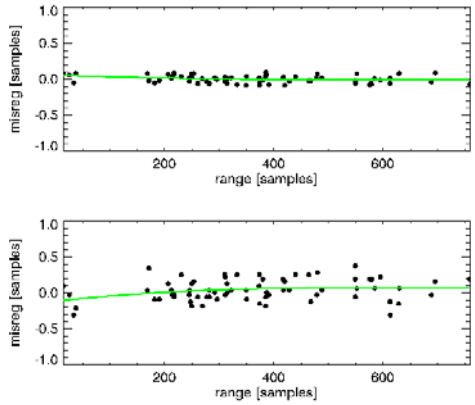

Fig. 3: Upper plot: misregistration in range and bottom plot: misregistration in azimuth both over slant range in the azimuth scene centre; The green line describes the misregistration of the actual SLC and the spread of the black dots indicates the coregistration precision of the overall data stack

3 TYPICAL ESTIMATION PRECISION

The typical estimation precision is defined as the standard deviation of the deformation measurement the end user can expect exchanging the OSP with its processing system i.e. the estimator (blue box) in Fig. 1 and Fig. 2 on a representative test site. DLR's validation approach using the PSI GENESIS system as a reference provides this information and clears the question on systematic effects (e.g. biases and algorithmic deficiencies) and excludes these.

The deformation measurement points (i.e. the PSs) are given by chance – but most importantly their quality (i.e. phase stability) varies on a given test site. Nearly ideal scatterers e.g. metal structures like trihedral or dihedral corner reflectors are rarely given. However the availability of usable scatterers improves if more deterioration in the phase stability is tolerated. The consequence is that the estimation quality varies spatially in a particular test site. Fig. 4 visualises the relation between the decreasing PS quality and the decreasing measurement precision. Shown are the scatter plots taken from two independent estimations of deformation measurements for different levels of phase stability of the PSs. The quality of the scatterers decreases from the upper left to the lower right and the non systematic deviation increases indicated by the broadened cloud of measurements (indicated by the red ellipses). The standard deviation of the deformation measurement is measured by sorting and grouping the estimates according to their coherence. The typical relation (i.e. all OSPs confirm it) between the coherence and the deformation standard deviation is plotted in Fig. 5. The best scatterers have a coherence of 0.97 and result in a deformation measurement standard deviation of 0.35 mm/year.

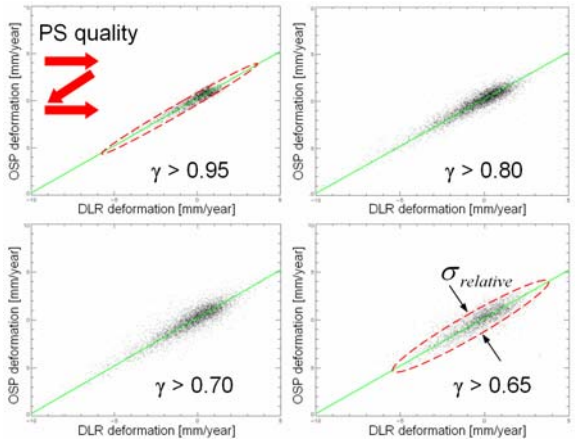

Fig. 4: Visualisation of the measured relation between the decreasing PS quality (from top left to bottom right) and the decreasing measurement precision indicated by the broadened scatter plot of deformation estimates from two independent PSI systems.

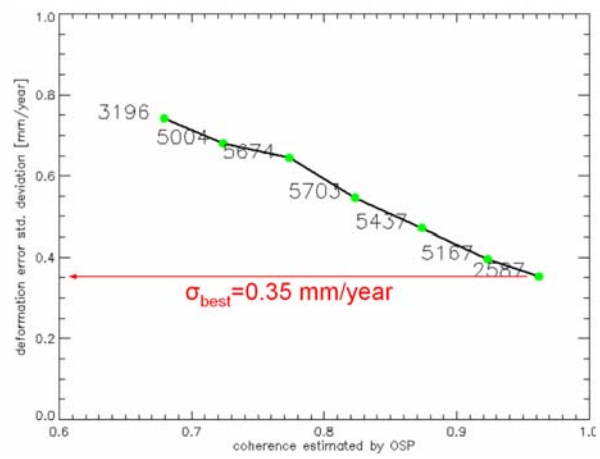

Fig. 5: Typical relation between the PS phase stability (indicated by the coherence) and the measured (green dots) deformation standard deviation between two independent estimations. (The number near the green dots is the sample size to estimate the std. deviation)

4 BEST POSSIBLE ESTIMATION PRECISION

The previous precision values are measured on practically available real scatterers. The measured linear relation between the coherence and the deformation standard deviation suggests to predict the estimation precision for optimal scatterers. Such scatterers are described by a temporal coherence of 1.0 which in practice can not be observed. These scatters need to have an infinite SCR and at the same time a linear displacement history over the full observation time span. Fig. 6 visualises the applied assumption of a linear dependency and the resulting limit in the deformation precision of 0.3 mm/year. Reference [6] provides another InSAR LOS precision measurement for optimal scatterers.

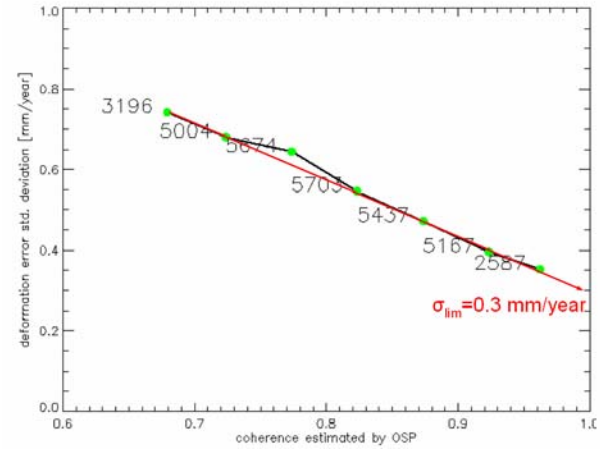

Fig. 6: 0.3 mm/year is the prediction of the deformation estimation precision for a theoretically ideal scatterer

5 THEORETICAL ABSOLUTE ESTIMATION PRECISON

The previous precision estimates are derived from two independent PSI processing chains and need to be considered a relative precision. Assuming both processings have the same error contribution, the absolute estimation precision σ_{PSI} is $1/\sqrt{2}$ of the measured relative standard deviation. I.e. the best measured absolute deformation standard deviation is 0.25 mm/year and the predicted absolute standard deviation for an ideal scatterer is approximately

$$\sigma_{PSI} = 0.21 \text{ [mm/year]}. \qquad (1)$$

These estimates can be confronted with the theory. Reference [7] provides an estimation precision estimate for the DEM update and the APS. Here, the relation between the deformation standard deviation and the coherence is approximated for high SCR. The coherence describes the output power resulting from the considered signal which is influenced by additional noise. The coherence is therefore described by the signal to noise ratio (SNR) which is replaced by the signal to clutter ratio (SCR):

$$\gamma = \frac{1}{1+\frac{1}{SCR}} \qquad (2)$$

The phase noise of a single PS observation can be approximated for high SCR by:

$$\sigma_{\varphi_{SLC}} = \frac{1}{\sqrt{2 \cdot SCR}} \qquad (3)$$

Reference [8] provides another approximation and the exact phase error probability density function related to the SCR. Eq. 2 describes the phase error of a particular acquisition. Assuming that the SCR is constant over time the interferometric phase standard deviation is:

$$\sigma_{\varphi_{INSAR}} = \sqrt{2\sigma^2_{\varphi_{SLC}}} = \frac{1}{\sqrt{SCR}} \qquad (4)$$

Similar to [7] the regression estimation is used instead of a frequency estimation to derive the estimation error. I.e. a line is fitted to the interferometric phase measurements φ_i and the displacement rate to phase conversion factors t_i with units *rad/(mm/year)*.

$$t_i = \frac{4 \cdot \pi[rad] \cdot T_i[days]}{\lambda[mm] \cdot 365[days/year]} = k \cdot T_i \quad (5)$$

T_i describes the time span between the master and the i-th slave acquisition i.e. for the i-th interferogram. The standard deviation of the estimated displacement rate is:

$$\sigma_{defo} = \sqrt{\frac{N_{free} \cdot \sigma^2_{\varphi_{INSAR}}}{S}} \quad (6)$$

N_{free} is the number of available interferograms N_{INSAR} corrected for the two lost degree of freedom due to the topography and APS estimation. *S* is provided by the regression theory:

$$S = N_{free} \cdot \sum_{i=1}^{N_{INSAR}} t_i^2 - \left(\sum_{i=1}^{N_{INSAR}} t_i \right)^2 \quad (7)$$

It can be simplified into

$$S = N_{free}^2 \cdot k^2 \cdot Var\{T_i\} = N_{free}^2 \cdot k^2 \cdot \frac{\Delta T^2}{12} \quad (8)$$

while the second term assumes a uniform distribution of acquisitions over an observation time span ΔT. Fig. 7 visualizes the standard deviation of the estimated displacement rate from Eq.5 for the Amsterdam test site (i.e. 38 interferograms (N_{INSAR}) and 4 years observation time (ΔT)) and the measured absolute deformation standard deviation.

Two effects can be observed: On the one hand, there is an offset of about 0.08 mm/year and on the other hand the non-linear finally infinitely steep slope is not measured. Both can be explained by the two facts that firstly the PSI estimation is in principle a relative measurement regarding a reference point and secondly an inherent non-avoidable noise floor σ_{floor} needs to be considered in practice and the measurable standard deviation σ_{PSI} is described by:

$$\sigma_{PSI} = \sqrt{\sigma^2_{defo}(\gamma) + \sigma^2_{floor}} \quad (9)$$

The noise floor prevents the optimal coherence of 1.0 being measured and is the sum of the variances of e.g. the following random effects:

- thermal noise in the radar sensor,
- focussing phase noise (can be detected by a phase offset alike test between SAR processors and is in the order of 5 degree),
- coregistration errors,
- interpolation errors and
- APS modelling by a spatial low pass signal.

For the single PS measurement this noise is included into the coherence estimate. But the integration of the relative estimates into the absolute values applying an integration constant (i.e. the reference point) results in Eq.9. I.e. the unavoidable use of a real ($SCR \neq \infty$ e.g. $\gamma_{ref} \cong \gamma_{floor}$) reference point adds the noise floor inherent in the interferometric phase and has been measured or predicted for an ideal scatterer at the beginning of this section (Eq. 1)

$$\sigma_{floor} = \sqrt{\sigma^2_{radar} + \sigma^2_{focus} + \sigma^2_{coreg} + \sigma^2_{approx} \cdots} = 0.21\ [mm/year] \quad (10)$$

Fig. 8 compares the theoretically measurable standard deviation σ_{PSI} from Eq.9 with the experimentally measured absolute deformation standard deviation.

The possible decomposition of the error terms into a scatterer related $\sigma_{defo}(\gamma)$ and an algorithmic or approximation caused error σ_{floor} describes the two possible future PSI improvements and the possible gains in estimation precision: Firstly, the scatterer related estimation error can be reduced using more ideal scatterers as e.g. corner reflectors or radar sensors with an improved resolution because both directly affect the SCR. Secondly, algorithmic improvements and optimized radar sensors can reduce the noise floor in the interferometric phase.

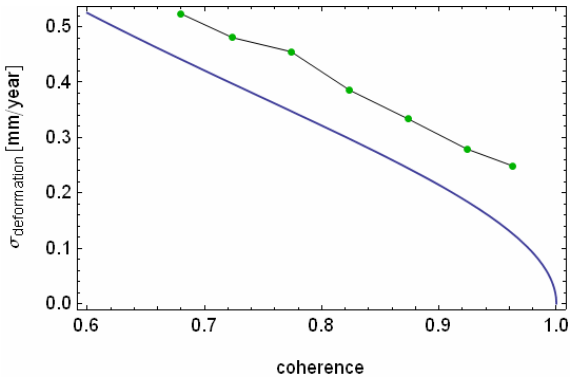

Fig. 7: blue line: theoretical deformation standard deviation of a single PS for the Amsterdam test site (observation time span 4 years, linear displacement only); green dots with black line: measured absolute deformation standard deviation σ_{PSI}.

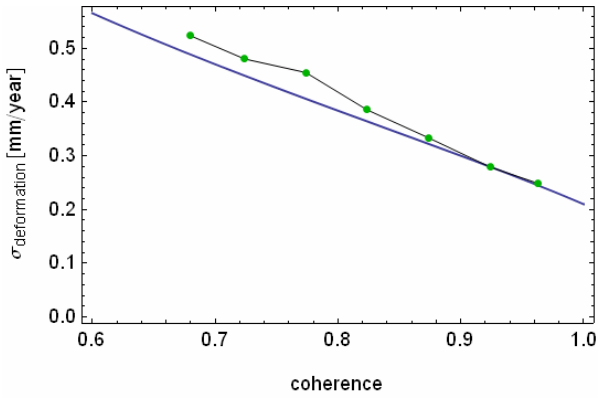

Fig. 8: blue line: theoretical deformation standard deviation of a single PS corrected for the not avoidable noise floor (Amsterdam test site); green dots with black line: measured absolute deformation standard deviation.

6 VALIDATION PROCEDURE

The Terrafirma validation procedure results in a qualification of the participating OSPs with respect to a level 1 product which is the PSI deformation measurement. A typical user expects two different types of information:

- a detection of risk (i.e. deformation) areas and
- a measurement of the deformation rate (e.g. an average velocity or a time series plot).

The validation procedure covers both requirements.

The detection is checked by a visual inspection of two significant displacement areas which are defined by the validation team. A risk area is considered detectable if it is

- covered by a typical number of PS,
- a linear deformation rate can be estimated,
- the estimated deformation is more than 2 mm/year,
- a clear shape of the deformation area can be described and
- the detection is confirmed by another independent PSI estimation.

Fig. 10 provides exemplarily the areas to be detected in the Amsterdam test site using this sort of slant range visualisation.

The deformation measurement is checked regarding a reference processing, i.e. a relative precision is measured. In principle every processing system which is free of systematic effects can be used as a reference. In the course of the validation, DLR's PSI GENSIS system has proven to fulfil this requirement and is used to check the standard deviation of the average displacement to be better or in the order of 1 mm/year. The precision estimation is based on the best 10000 measurements according the delivered OSP's coherence, because the quality of the scatterers inside of a test site varies.

The use of three different test sites helps to separate processing system and system operator effects. All three test sites are used for the OSP's validation according to the validation procedure described above. However only the best processing (i.e. one test site) is finally used to check for the applicable detection and precision benchmarks.

7 CONCLUSIONS

The PSI process validation in slant range domain provides the precision estimate for actual PSI processing chains over a typical test site using the sensors ERS or Envisat ASAR. This precision varies spatially depending on the scatterer's SCR. The practical deformation precision depending on the estimated coherence is measured and predicted for an optimal scatterer. These measurements are compared with the theory. The deformation estimation is limited by an inherent noise floor in the interferometric phase caused e.g. by the radar's thermal noise, the focussing and the coregistration. This limit is measured to be currently 0.21 mm/year linear deformation standard deviation for a typical Envisat ASAR or ERS test site with an observation time span of about four years using DLR's PSI-GENESIS system as a reference.
The applied assessment procedure allows the detection of systematic effects. No bias or other systematic effects are found in a typical PSI processing. Terrafirma's test sites are perfectly suitable for the validation of PSI chains.

ACKNOWLEDGEMENTS We acknowledge the support by ESA and the PSI intermediate data contribution of Altamira Information, Gamma RS, NPA and Tele-Rilevamento Europa (T.R.E.) in the framework of the Terrafirma project.

5 REFERENCES

1 Crosetto M., M. Agudo, C. Bremmer, R. Hanssen, (2007). Technical note on the test site selection: Alkmaar-Amsterdam.
2 Crosetto M., Agudo M., Adam N. (2007). General Rules to Run the Validation Project, Issue. 5
3 Adam N., Parizzi A. (2007). Specification of Validation Approach Part 1: Process Validation, Issue 1.8.
4 Rosich Tell B., Laur H. (1996). Phase Preservation in SAR Processing: the Interferometric Offset Test. IGARSS96, Lincoln, Nebraska, USA, 27-31.
5. Adam N, Bamler R, Eineder M, Kampes B (2005). Parametric estimation and model selection based on

amplitude-only data in PS-interferometry. Proceedings of FRINGE'05, Frascati, Italy, on CD.
6. Ferretti A., G. Savio, R. Barzaghi, A. Borghi, S. Musazzi, F. Novali, C. Prati, F. Rocca (2007). Submillimeter Accuracy of InSAR Time Series: Experimental Validation. IEEE TGaRS, Vol. 45, N. 5; 1142-1153.
7. Rocca F. (2004). Diameters of the Orbital Tubes in Long-Term Interferometric SAR Surveys. IEEE GaRSL, vol. 1, 224-227.
8. Adam N, Kampes B.M., Eineder M (2004) The development of a scientific persistent scatterer system: Modifications for mixed ERS/ENVISAT time series. ENVISAT/ERS Symposium.

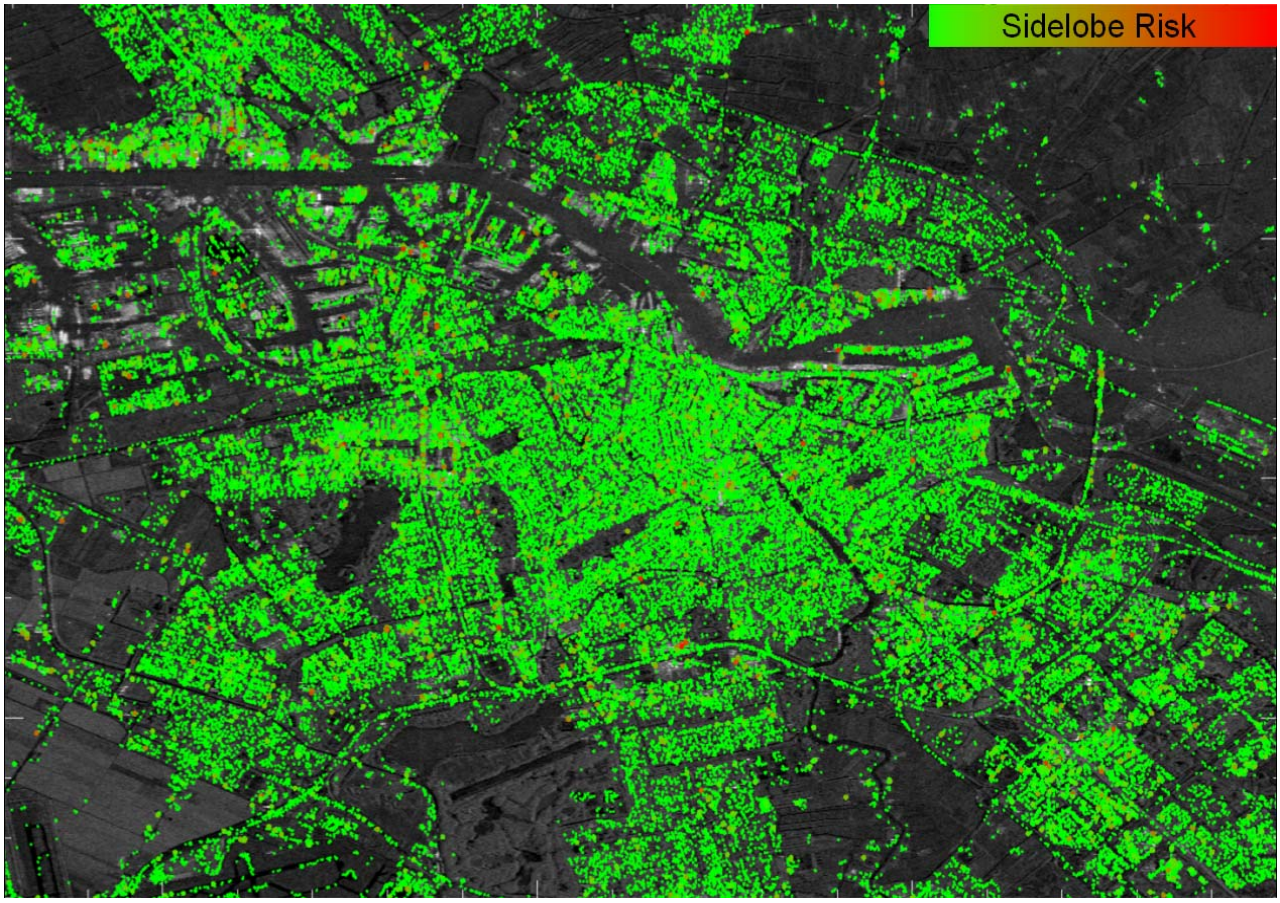

Fig. 9: Overlay of the radar mean intensity image and the detected PS in the Amsterdam ASAR test site. Red indicates detected PS with a high risk to be sidelobes. The number of risky PS is insignificant.

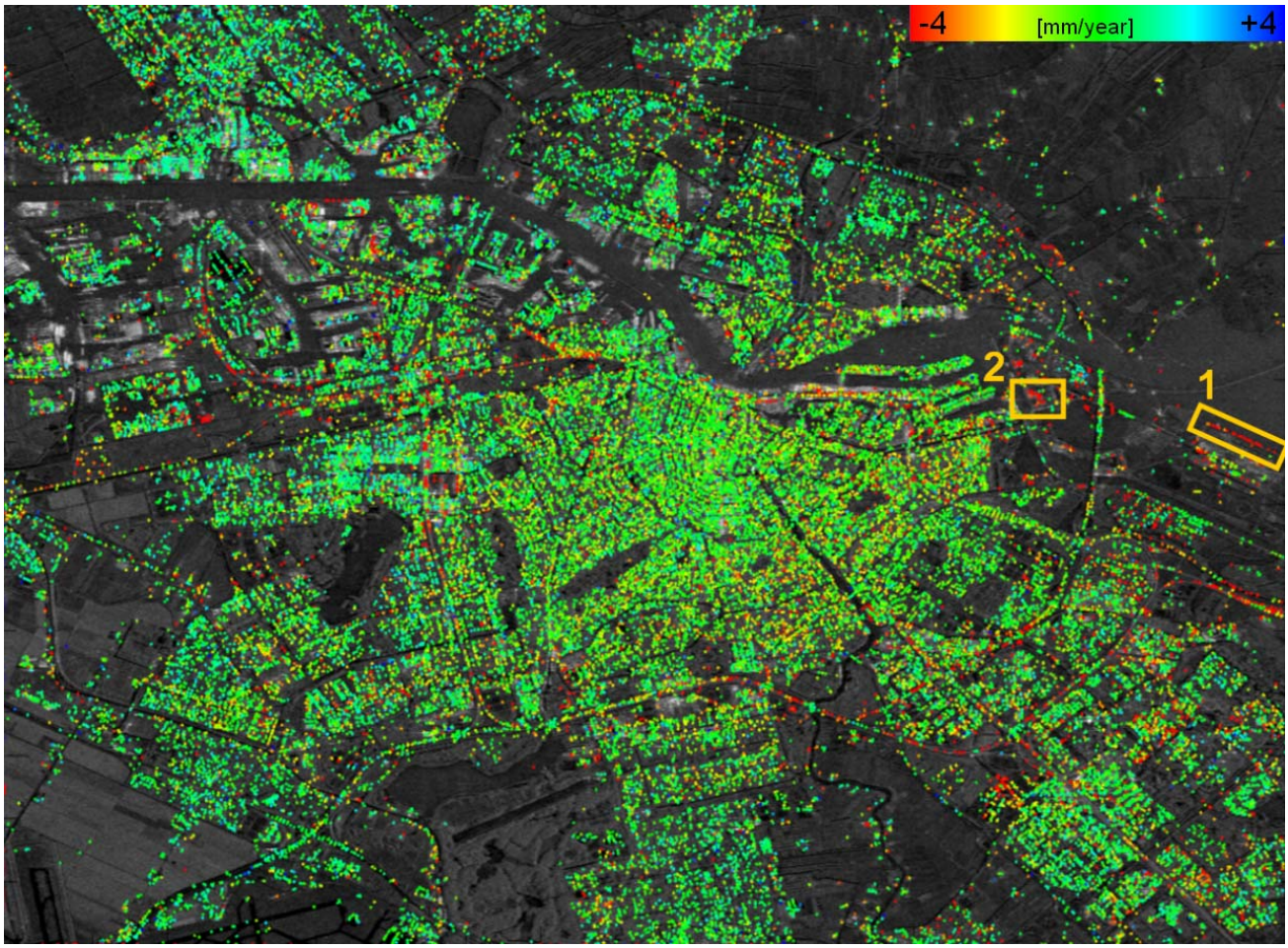

Fig. 10: Deformation estimation map showing the proposed areas to check the detection in the Amsterdam test site